

# New 1,3,4-thiadiazole compounds: synthesis, spectroscopic characterisation and theoretical analyses based on DFT calculations

Muhammet Serdar ÇAVUŞ<sup>1,\*</sup>, Halit MUĞLU<sup>2</sup>

<sup>1</sup> Kastamonu University, Faculty of Engineering and Architecture, Department of Biomedical Engineering, Kuzeykent Campus, Kastamonu.

<sup>2</sup> Kastamonu University, Faculty of Art and Science Department of Chemistry, Kuzeykent Campus, Kastamonu.

Geliş Tarihi (Recived Date): 23.11.2017  
Kabul Tarihi (Accepted Date): 17.01.2018

## Abstract

*In this study, four novel 1,3,4-thiadiazole compounds, derived from  $\alpha$ -methyl cinnamic acid, were synthesised. The structural elucidation was carried out using UV-Vis, FT-IR, <sup>1</sup>H-NMR and <sup>13</sup>C-NMR spectroscopy. In addition, the chemical and electronic properties of the compounds as well as UV-Vis, IR and NMR analyses were theoretically performed using the density functional theory (DFT). Based on the frontier molecular orbital (FMO) energies of the compounds, which were obtained from different methods and basis sets, some chemical reactivity parameters and their relationship with the methods were analysed. Theoretical calculations were compared with the experimental results. The electronegative substituents Cl and NO<sub>2</sub> reduced the HOMO–LUMO energy gap ( $\Delta E$ ), and the ones caused a bathochromic shift in the UV absorption wavelength. The Pearson correlation coefficients between the experimental and theoretical IR and <sup>13</sup>C NMR results were approximately  $R = 0.99$ . It was seen that, the chemical shift of hydrogen bound to an electronegative nitrogen atom was affected by intramolecular hydrogen bond interactions.*

**Keywords:** 1,3,4-thiadiazoles,  $\alpha$ -methyl cinnamic acid, computational chemistry, density functional theory.

---

\* Muhammet Serdar ÇAVUŞ, mserdarcavus@kastamonu.edu.tr, <http://orcid.org/0000-0002-3721-0883>  
Halit MUĞLU, hmuglu@kastamonu.edu.tr, <http://orcid.org/0000-0001-8306-2378>

## Yeni 1,3,4-tiadiazol bileşikleri: sentez, spektroskopik karakterizasyon ve DFT hesaplamalarına dayanan teorik analizler

### Özet

*Bu çalışmada,  $\alpha$ -metil sinnamik asitten türetilen dört yeni 1,3,4-tiadiazol bileşiği sentezlendi. Bileşiklerin yapısal özellikleri UV-Vis, FT-IR,  $^1\text{H-NMR}$  ve  $^{13}\text{C-NMR}$  spektroskopisi kullanılarak incelendi. Buna ek olarak, bileşiklerin kimyasal ve elektronik özelliklerinin yanı sıra UV-Vis, IR ve NMR analizleri teorik olarak yoğunluk fonksiyonel teorisi (DFT) kullanılarak gerçekleştirildi. Farklı yöntemler ve baz setleri kullanılarak elde edilen, bileşiklerin sınır moleküler orbital (FMO) enerjilerine dayanılarak, bazı kimyasal reaksiyon parametreleri ve bunların kullanılan yöntemlerle ilişkisi analiz edildi. Teorik hesaplamalar deney sonuçları ile karşılaştırıldı. Elektronegatif Cl ve NO<sub>2</sub> süstitüentlerinin HOMO-LUMO enerji aralığını ( $\Delta E$ ) düşürdüğü ve UV-absorbsiyon dalga boyunda bir batokromik kaymaya neden olduğu gözlemlendi. Deneysel ve teorik IR ve  $^{13}\text{C}$  NMR sonuçları arasındaki Pearson korelasyon katsayıları yaklaşık olarak  $R = 0.99$  olarak hesaplandı. Elektronegatif azot atomuna bağlı hidrojenin kimyasal kaymasının, molekül içi hidrojen bağı etkileşimlerinden etkilendiği gözlemlendi.*

**Anahtar kelimeler:** 1,3,4-tiadiazol,  $\alpha$ -metil sinnamik asit, hesaplamalı kimya, yoğunluk fonksiyonel teorisi.

### 1. Introduction

Heterocyclic compounds have great importance in many fields such as organic, pharmaceutical and biochemistry. One of the most important compounds in this field, i.e., 1,3,4-thiadiazole derivatives, are five-membered heterocyclic compounds containing one sulfur and two nitrogen atoms [1]. These derivatives are used in a wide variety of fields such as the pharmaceutical industry, materials science and organic synthesis [2]. Recently, a great variety of 1,3,4-thiadiazoles, to which aromatic moieties with different substituents are attached, have been intensively investigated. In the analytical, biological and pharmaceutical fields, these derivatives are the most interesting isomeric form of the thiadiazole compounds [3,4]. The N=C-S moiety in the thiadiazole ring results in numerous biological and pharmaceutical activities such as anti-glaucoma, anti-inflammatory, anti-tumour, anti-ulcer, anti-bacterial, anti-viral, analgesic, anti-epileptic, anti-fungal and radio-protective properties. Furthermore, the aromaticity of the thiadiazoles contributes to a decreased toxicity and an improved durability in the living organism [5]. Many methods have been described for the synthesis of 1,3,4-thiadiazole compounds, where the most common starting materials are as follows: thiosemicarbazites, thiocarbazides, dithiocarbazates, thioacylhydrazines, acylhydrazines and bitolyure derivatives [6-14]. Furthermore, some of the properties of thiadiazole and its derivatives have been successfully studied using quantum mechanical calculations [15-20]. In this study, four new 1,3,4-thiadiazole compounds were synthesised and the structures of the compounds were elucidated using a variety of spectroscopic methods (FT-IR,  $^1\text{H}$  NMR and UV-Vis). In addition to the synthesis and structural elucidation, the UV, IR and NMR spectra and the frontier molecular orbitals (FMO) characteristics of the compounds were theoretically examined to support the

experimental studies. Particularly, the molecular and electronic properties as well as the UV-Vis absorption domains, IR vibration frequencies and NMR peak values were theoretically calculated and analysed.

## 2. Methods

### 2.1. Synthesis

#### 5-(1-Methyl-2-phenylethenyl)-N-[2',4'-dichlorophenyl]-1,3,4-thiadiazol-2-amine (I)

The general method for the synthesis of the 1,3,4-thiadiazole derivatives was as follows.  $\alpha$ -Methyl cinnamic acid (n mol) and the corresponding N-substituted-phenylthiosemicarbazide derivatives (n mol) were placed into a refrigerator, and then phosphorous oxychloride (3n mol) was added drop-wise to the cold mixture while stirring and the reflux was continued for two hours. Once the reaction was complete, the reaction flask was cooled to the room temperature and the crude product was added to ice-cold water while stirring. This mixture was neutralised with an ammonia solution. The precipitated product was filtrated, washed with water and crystallised using different solvents such as ethanol and tetrahydrofuran (THF). The spectral data of the compounds are summarised in Tables 1–4.

Yield%: (%76), M.P.: 160 °C; **FT-IR** ( $\text{cm}^{-1}$ )  $\nu_{\text{maks}}$ : 3285.01 (-NH stretching), 1495.65 (-NH bending), 3055.61 (aromatic C-H), 2961.91, 2918.67 (aliphatic C-H), 1597.51 (C=N thiadiazole), 1610 (C=C) 698.56 (C-S-C):  **$^1\text{H-NMR}$  (400 MHz, DMSO- $d_6$ , 25 °C)  $\delta$  (ppm)**: 2.47 (s, 3H -CH<sub>3</sub>), 7.25-7.46 (8H, aromatic), 8.40 (g, -NH), 7,11 (s, 1H, ethylenic);  **$^{13}\text{C-NMR}$  (DMSO- $d_6$ , 25 °C)  $\delta$  (ppm)**: (in order of C1-C17), 135.94, 129.19, 127.98, 128.47, 127.98, 129.19, 119.74, 122.79, 15.92, 162.90, 163.77, 129.46, 135.23, 136.19, 135.23, 128.21, 129.40. **Elemental analysis**: Anal. Calcd. for C<sub>17</sub>H<sub>13</sub>Cl<sub>2</sub>N<sub>3</sub>S: C, 56.36; H, 3.62; N, 11.60 (%). Found: C, 58.03; H, 3.44; N, 11.23 (%). The synthetic route and general structure of the molecules are illustrated Figure 1.

#### 5-(1-Methyl-2-phenylethenyl)-N-[4'-nitrophenyl]-1,3,4-Thiadiazol-2-amine (II)

Yield%: (%67), M.P.: 166 °C **FT-IR** ( $\text{cm}^{-1}$ )  $\nu_{\text{maks}}$ : 3218.45 (-NH, stretching), 1495.63 (-NH, bending), 3044.94 (aromatic C-H), 2981.48, 2903.17, 2811.16 (aliphatic C-H), 1597.99 (C=N thiadiazole), 1626.58 (C=C) 709.96 (C-S-C):  **$^1\text{H-NMR}$  (400 MHz, DMSO- $d_6$ , 25 °C)  $\delta$  (ppm)**: 2.51 (s, 3H -CH<sub>3</sub>), 7.34-8.27 (9H, aromatic), 11.28 (g, -NH), 7.22 (s, 1H, ethylenic):  **$^{13}\text{C-NMR}$  (DMSO- $d_6$ , 25 °C)  $\delta$  (ppm)**: (in order of C1-C17), 136.21, 134.26, 129.26, 129.92, 129.26, 134.26, 125.98, 128.93, 16.13, 162.74, 163.83, 146.67, 117.54, 128.41, 141.37, 128.41, 117.54. **Elemental analysis**: Anal. Calcd. for C<sub>17</sub>H<sub>14</sub>N<sub>4</sub>O<sub>2</sub>S: C, 60.34; H, 4.17; N, 16.56 (%). Found: C, 58.91; H, 3.87; N, 15.38 (%).

#### 5-(1-Methyl-2-phenylethenyl)-N-[phenylmethyl]-1,3,4-Thiadiazol-2-amine (III)

Yield%: (% 63), M.P.: 217 °C **FT-IR** ( $\text{cm}^{-1}$ )  $\nu_{\text{maks}}$ : 3191.26 (-NH stretching), 1491.69 (-NH, bending), 3078.51 (aromatic C-H), 2981.71, 2964.53, 2869.72 (aliphatic C-H), 1572.37 (C=N thiadiazole), 1601.00 (C=C) 693.70 (C-S-C):  **$^1\text{H-NMR}$  (400 MHz, DMSO- $d_6$ , 25 °C)  $\delta$  (ppm)**: 2.40 (s, 3H -CH<sub>3</sub>) 4.58 (s, 2H -CH<sub>2</sub>-), 7.29-7.41 (10H, aromatic), 9.01 (g, -NH), 6.96 (s, 1H, ethylenic);  **$^{13}\text{C-NMR}$  (DMSO- $d_6$ , 25 °C)  $\delta$  (ppm)**: (in order of C1-C18), 136.33, 130.05, 127.78, 129.31, 127.78, 130.05, 127.56, 132.47, 15.83, 161.93, 169.01, 137.01, 128.86, 128.36,

127.99, 128.36, 128.86, 50.68. **Elemental analysis:** Anal. Calcd. for C<sub>18</sub>H<sub>17</sub>N<sub>3</sub>S: C, 70.33; H, 5.57; N, 13.67 (%). Found: C, 68.58; H, 5.43; N, 12.85 (%).

*5-(1-Methyl-2-phenylethenyl)-N-[2'-phenylethyl]-1,3,4-Thiadiazol-2-amine (IV)*

Yield%: (%67), M.P.: 160 °C; **FT-IR (cm<sup>-1</sup>)**  $\nu_{\text{maks}}$ : 3153.16 (-NH stretching), 1486.07 (-NH, bending), 3056.38 (aromatic C-H), 2964.56, 2804.66 (aliphatic C-H), 1580.00 (C=N thiadiazole), 1620.99 (C=C) 695.72 (C-S-C): **<sup>1</sup>H-NMR (400 MHz, DMSO-d<sub>6</sub>, 25 °C)  $\delta$  (ppm):** 2.27 (s, 3H -CH<sub>3</sub>), 2.95 (t, 2H -CH<sub>2</sub>-), 3.69 (t, 2H -CH<sub>2</sub>-), 7.23-7.50 (10H, aromatic), 9.94 (g, -NH), 7.09 (s, 1H, ethylenic); **<sup>13</sup>C-NMR (DMSO-d<sub>6</sub>, 25 °C)  $\delta$  (ppm):** (in order of C1-C18), 134.39, 129.31, 128.72, 128.87, 128.72, 129.31, 126.87, 129.96, 15.64, 159.56, 167.20, 135.93, 128.57, 128.94, 126.88, 128.94, 128.57, (47.16 and 34.52). **Elemental analysis:** Anal. Calcd. for C<sub>19</sub>H<sub>19</sub>N<sub>3</sub>S: C, 71.00; H, 5.96; N, 13.07 (%). Found: C, 69.95; H, 5.40; N, 12.85 (%).

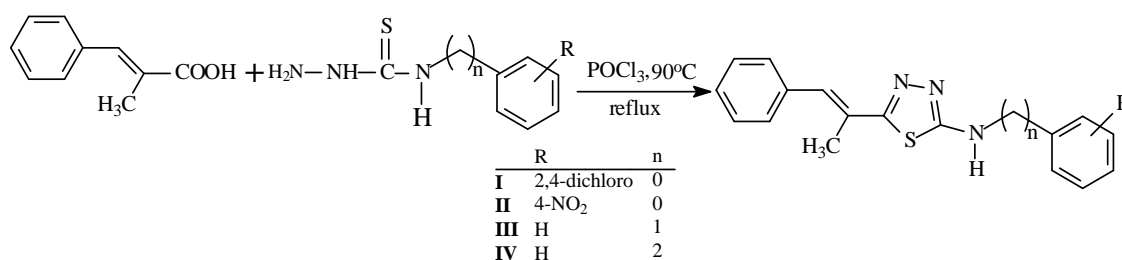


Figure 1. Synthesis of the 1,3,4-thiadiazole compounds

### 3. Results and Discussion

#### 3.1. FT-IR Spectroscopy

The IR absorption data of the obtained compounds (I–IV) are presented in Table 1. The structural characterisation was performed based on the IR absorptions of the –NH, –C–H (aromatic and aliphatic), –C=N (thiadiazole ring), –C=C– and C–S–C functional groups. It has been reported that the secondary amine group (–NH–) has a stretching and a bending vibration at 3350–3310 and 1580–1490 cm<sup>-1</sup>, respectively. In addition, the stretching vibrations of C=N, aromatic C–H, aliphatic C–H and aromatic C=C are respectively reported in the following ranges: 1689–1471, 3100–3000, 3000–2840 and 1650–1450 cm<sup>-1</sup>. Moreover, the peaks belonging to the conjugated C=C and C–S–C are found at around 1645 and 700 cm<sup>-1</sup> [1, 2].

For the compounds I–IV, the vibrations of the N–H stretching, N–H bending, aromatic C–H stretching, aliphatic C–H stretching, –C=N stretching (thiadiazole ring), C–S–C and C=C were determined at 3285.01–3153.16, 1495.65–1486.07, 3078.51–3044.94, 2981.71–2804.66, 1597.99–1572.37, 709.96–693.70 and 1626.58–1601.00 cm<sup>-1</sup>, respectively. Further proof of the conversion of  $\alpha$ -methylcinnamic acid to the thiadiazole was the absence of the >C=O peak, which is usually strong and located from 1750 to 1700 cm<sup>-1</sup>. The presence of the secondary amine, C=N and C–S–C peaks, and the lack of absorption of the carbonyl group proved that the desired final products were successfully synthesised.

Table 1. Absorption data of compounds I–IV in the FT-IR region.

Compounds	$\nu_{(-N(H)-)}$	$\nu_{C-H}$ (Aromatic)	$\nu_{C-H}$ (aliphatic)	$\nu_{C=N}$ (thiadiazole)	$\nu_{C-S-C}$	$\nu_{(C=C)}$
I	3285.01 (stretching) 1495.65 (bending)	3055.61	2961.91 2918.67	1597.51	698.56	1610.00
II	3218.45 (stretching) 1495.63 (bending)	3044.94	2981.48 2903.17 2811.16	1597.99	709.96	1626.58
III	3191.26 (stretching) 1491.69 (bending)	3078.51	2981.71 2964.53 2869.72	1572.37	693.70	1601.00
IV	3153.16 (stretching) 1486.07 (bending)	3056.38	2964.56 2804.66	1580.00	695.72	1620.99

### 3.2. $^1H$ -NMR Spectroscopy

$^1H$ -NMR data of compounds I–IV are listed in Table 2. The synthesised compounds possess aromatic, aliphatic, alkenic and secondary amine protons. The determination of these  $^1H$ -NMR signals is important for the structural elucidation of the synthesised compounds. The aromatic protons were observed between 7.23 and 8.27 ppm. The protons of the  $-CH_3$  group bound to the alkene were located from 2.27 to 2.57 ppm (singlets). The protons of the aliphatic  $-CH_2$  and  $-CH_2-CH_2-$  groups in compounds III and IV were around 4.58 (s, 2H  $-CH_2-$ ), 2.95 (t, 2H  $-CH_2-$ ) and 3.69 (t, 2H  $-CH_2-$ ). The secondary amine protons were between 8.40 and 11.28 but the amine peak was not observed in III. The ethylenic proton shifted to the aromatic region due to the conjugation with the two aromatic rings and it was located in the range of 6.96–7.22 ppm.

Table 2.  $^1H$ -NMR data of compounds I–IV ( $\delta$ , ppm, DMSO- $d_6$ ).

Compounds	$\delta$ Aliphatic-H	$\delta$ Aromatic-H	$\delta$ N-H	$\delta$ ethylenic C-H
I	2.47 (s, 3H $-CH_3$ )	7.25-7.46 (8H, aromatic)	8.40 (g, -NH)	7.11 (s, 1H)
II	2.51 (s, 3H $-CH_3$ )	7.34-8.27 (9H, aromatic)	11.28 (g, -NH)	7.22 (s, 1H)
III	2.40 (s, 3H $-CH_3$ ) 4.58 (s, 2H $-CH_2-$ )	7.29-7.41 (10H, aromatic)	9.01 (g, -NH)	6.96 (s, 1H)
IV	2.27 (s, 3H $-CH_3$ ) 2.95 (t, 2H $-CH_2-$ ) 3.69 t, 2H $-CH_2-$ )	7.23-7.50 (10H, aromatic)	9.94 (g, -NH)	7.09 (s, 1H)

### 3.3. $^{13}C$ -NMR Spectroscopy

The  $^{13}C$ -NMR data of I–IV are given in Table 3. There were two types of aromatic C atoms in the compounds, the ones of the benzene ring and those of the thiadiazole. The electronegative N atom affected the C11 atom (adjacent to the secondary amine). Thus, it was downfield shifted and its signal was located between 163.77 and 169.01 ppm. Likewise, C10 was observed at 159.56–162.90 ppm. The phenyl carbons (C12–C17) adjacent to the secondary amine resonated in the 117.54–146.67 ppm range and the signals of the C atoms of the phenyl rings (C1–C6), adjacent to the alkene double bond, were at 127.78–136.33 ppm. The C atom ( $CH_3$ ) bound to the alkene structure was observed in the range of 15.64–16.13 ppm. The alkenic C7 and C8 atoms were respectively found in around 119.74–127.56 and 122.79–132.47 ppm. For compounds

III and IV, the C18 atoms were observed at 50.68 ppm and 47.16 and 34.52 ppm, respectively.

Table 3. <sup>13</sup>C-NMR data of compounds I–IV (δ, ppm, DMSO-d<sub>6</sub>).

Compounds:  
I: 2,2'-dichloro, II: 4-nitro,  
III: n = 1 and IV: n = 2

	I	II	III	IV
C <sub>1</sub>	135.94	136.21	136.33	134.39
C <sub>2</sub>	129.19	134.26	130.05	129.31
C <sub>3</sub>	127.98	129.26	127.78	128.72
C <sub>4</sub>	128.47	129.92	129.31	128.87
C <sub>5</sub>	127.98	129.26	127.78	128.72
C <sub>6</sub>	129.19	134.26	130.05	129.31
C <sub>7</sub>	119.74	125.98	127.56	126.87
C <sub>8</sub>	122.79	128.93	132.47	129.96
C <sub>9</sub>	15.92	16.13	15.83	15.64
C <sub>10</sub>	162.90	162.74	161.93	159.56
C <sub>11</sub>	163.77	163.83	169.01	167.20
C <sub>12</sub>	129.46	146.67	137.01	135.93
C <sub>13</sub>	135.23	117.54	128.86	128.57
C <sub>14</sub>	136.19	128.41	128.36	128.94
C <sub>15</sub>	135.23	141.37	127.99	126.88
C <sub>16</sub>	128.21	128.41	128.36	128.94
C <sub>17</sub>	129.40	117.54	128.86	128.57
C <sub>18</sub>	-	-	50.68	47.16, 34.52

### 3.4. UV-Vis Absorption

The UV-Visible absorption spectra of compounds I–IV were recorded in a 10<sup>-5</sup> M concentration, from 200 to 700 nm using chloroform as solvent. According to the results shown in Table 4, the absorption spectra of all compounds I-IV was found single peak without shoulder between 266 nm and 368,5 nm except for Compound I. therefore, we can say that these compounds have only one tautomeric form in CHCl<sub>3</sub>. The substituted compounds of the phenyl ring (comp. I and II) showed more bathochromic shift than the unsubstituted compounds (comp. I and II). Also when we compared compound 4 (where n is 2 in the structure) with compound 3 (where n is 1 in the structure), we saw that compound 4 showed hypsochromic shift.

Table 4. Experimental and theoretical UV-Vis absorptions of compounds I–IV (nm).

Compound	Experimental	Theoretical	
		B3PW91	B3LYP
I	266.00, 333.50	277.01, 357.76	277.67, 357.45
II	368.50	328.40, 405.57	333.43, 411.11
III	322.00	333.79	334.20
IV	310.50	337.16	339.77

### 3.5. Theoretical Calculations

In this work, the Kohn–Sham density functional theory (DFT) method [21, 22] was used for the quantum chemical calculations of the compounds. For the molecular optimization process, carried out as the first step of the theoretical calculations, no restrictions were set on the geometry of the compounds. The popular semi-empirical Becke3–Perdew–Wang91 (B3PW91) and Becke3–Lee–Yang–Parr hybrid functional (B3LYP) methods with a cc-pvtz basis set were separately used for the molecular optimizations. For each geometry, the minimum was confirmed by frequency calculations with no imaginary frequency. Furthermore, the methods mentioned above were used to obtain the ground state energies, molecular conformations and the UV-Vis, IR and NMR spectra of the compounds.

The initial conformations for the optimization calculations, the most suitable dihedral angles and bond lengths, among others, were obtained by scan procedures. In this processes, each of the compounds was dihedral-scanned around the thiadiazole moiety with a step size of  $36^\circ$  and  $60^\circ$  for a total of 60 steps (Fig. 2), using the B3LYP method with a 6-31 + g basis set to determine the minimum energy level configuration.

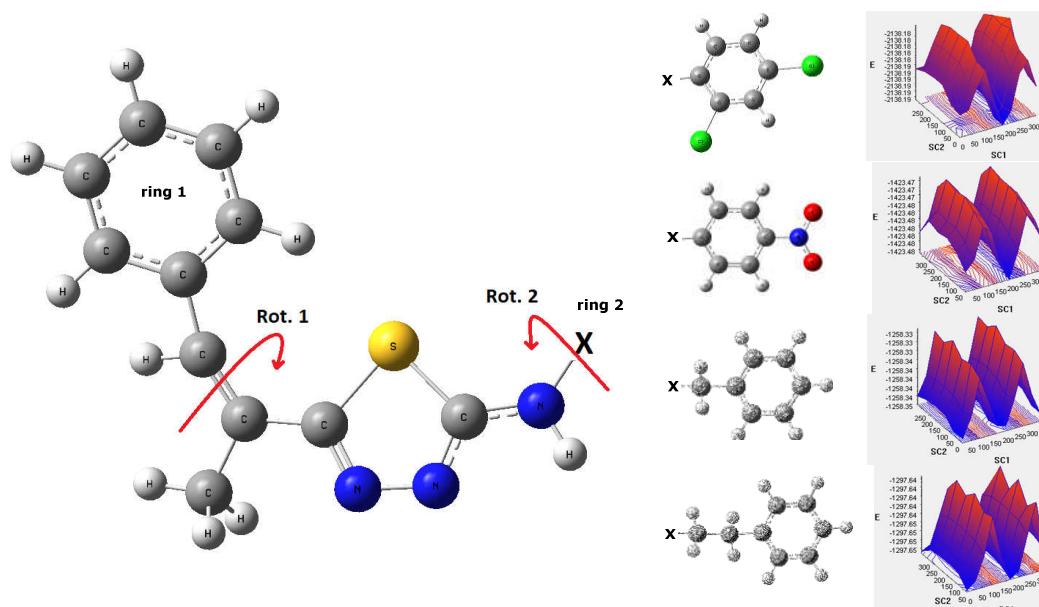


Figure 2. Dihedral scanning of compounds I–IV. Rotations and energy versus dihedral scan angles.

The UV-Vis absorption wavelengths were calculated in the chloroform phase using the same method and basis sets for optimised ground state geometries. The effects of the solvent were included by considering it as a continuum characterised by a dielectric constant using the self-consistent field reaction method (SCRF). The conductor-polarisable continuum model was used for the geometry optimizations and excited state energy calculations of all molecules in solvent media, the solvent and solute interactions were considered. Similarly, the theoretical gauge-invariant atomic orbital method, which is the most reliable and widely used method to compute nuclear magnetic shielding tensors, was used to compute the NMR chemical shifts of the compounds using the DFT/B3LYP and B3PW91 functionals with the cc-pvtz basis set in a dimethylsulfoxide (DMSO) phase according to the experimental procedure. Comparisons between the experimental and theoretical values of the NMR spectra were

used for the analysis of the most stable conformations calculated for each compound. Additionally, IR spectral data were obtained using the cc-PVTZ basis set by the methods described above in gas phase.

The highest occupied (HOMO) molecular orbitals energies, lowest unoccupied (LUMO) molecular orbitals energies and frontier molecular orbitals (FMOs) were calculated using the same methods and basis sets. Also, the molecular electrostatic potential surfaces were obtained. The FMO energy eigenvalues were used to calculate the chemical hardness ( $\eta$ ) and electronegativity ( $\chi$ ) of the compounds. All the calculations were performed using the GAUSSIAN 09 software [23].

The Cl and NO<sub>2</sub> functional groups of compounds I and II directly affected the chemical hardness and electronegativity of the compounds. Since the electronegativity of oxygen is greater than that of chlorine, the electronegativity of the NO<sub>2</sub> substituted compound (II, 4.44 eV) is also greater than that of the Cl compound (I, 3.90 eV), using B3LYP/cc-pvtz. The chemical stiffness of II is lower than that of I because the electronegativity of II is greater. Moreover, the electronegativity of the substituents affected the LUMO energies and reduced the value of  $\Delta E$ , thus the chemical hardness inversely decreased with respect to electronegativity. In addition, there is a correlation between the electron affinity of the functional groups and the dipole moments of the compounds. As the molecular electron density of the electronegative substituents (Cl, N and O) increased, the compounds showed a larger electronic polarisability. This resulted in a larger dipole moment for the functional groups with higher electronegativity (3.8 D for II and 2.9 D for I). Compounds III and IV presented similar results. The positive CH<sub>2</sub> decreased the dipole moment of IV compared to III. In addition, both the chemical stiffness and electronegativity of compound IV were lower than those of III. The binding of the positive CH<sub>2</sub> to compound III affected the HOMO energy of this compound. An analogous effect of the electronegativity of the substituents was observed for compounds III and IV (Table 5).

Table 5. Electrochemical calculations of compounds I–IV.

Compound	Method	$E$ (au)	$E_{\text{HOMO}}$ (eV)	$E_{\text{LUMO}}$ (eV)	$\Delta E$ (eV)	$\eta$ (eV)	$\chi$ (eV)	$m$ (Debye)
I	B3PW91 (cc-pvtz)	-2138.350691	-5,963	-1,878	4,085	2,042	3,921	2.907
II		-1423.695031	-6,277	-2,621	3,656	1,828	4,449	3.823
III		-1258.501921	-5,811	-1,554	4,257	2,128	3,682	3.999
IV		-1297.816236	-5,791	-1,549	4,243	2,121	3,670	3.812
I	B3LYP (cc-pvtz)	-2138.830489	-5,942	-1,859	4,083	2,041	3,901	2.963
II		-1424.150240	-6,249	-2,632	3,617	1,809	4,440	3.892
III		-1258.894405	-5,789	-1,532	4,257	2,128	3,661	4.018
IV		-1298.223527	-5,776	-1,531	4,245	2,122	3,654	3.832

$E$ : Energy,  $\Delta E$ :  $E_{\text{LUMO}} - E_{\text{HOMO}}$ ,  $\eta$ : Chemical Hardness,  $\chi$ : Electronegativity,  $m$ : Dipole moment

The vibrational harmonic frequencies of the compounds were calculated using the same level of theory and basis set than for the geometry optimization. The absence of imaginary frequencies assessed that the optimised structures were the minimum, in other words, the calculated optimizations corresponded to the minimum point of the intramolecular potential energy surface. The results of the theoretical IR calculations were consistent with the experimental data. Selected experimental and theoretical vibrational frequencies are reported in Table 6.

It is known that the Pearson correlation coefficient measures the linear dependence between two random variables. The correlation coefficients (R) of the mean values of the experimental and theoretical oscillation frequencies were 0.9941 and 0.9932 for B3LYP and B3PW91, respectively. These R-values showed the high correspondence between the experimental and theoretical data. Furthermore, as seen in Figure 3, the linear regression analysis revealed the relationship between the experimental ( $x$ ) and theoretical ( $y$ ) results:  $y = 1.135x - 186.5$  and  $y = 1.136x - 176.6$  for B3LYP and B3PW91, respectively. Although the theoretical and experimental IR results were similar, the calculated N–H and aromatic and aliphatic =C–H bond vibrations were higher than the experimentally determined values because the theoretical calculations were performed for single molecules, i.e., the intermolecular interactions were not considered.

Table 6. Theoretical and experimental IR vibrational frequencies of compounds I–IV ( $\text{cm}^{-1}$ ).

Method	Comp.	$\nu_{\text{N(H)}}$	$\nu_{\text{C-H}}$ (Aromatic)	$\nu_{\text{C-H}}$ (aliphatic)	$\nu_{\text{C=C}}$	$\nu_{\text{C=N}}$ (thiadiazole)	$\nu_{\text{C-S-C}}$	
B3LYP /cc-pvtz	I	3549.89 (stretching)	3193.14 r1 ss	3128.39	1679.78	1568.95	665.16	
		1419.74 (bending)	3184.71 r1 as					
			3177.57 r1 as					
	II	3572.86 (stretching)	3193.83 r1 ss	3128.65	1679.81	1590.05	680.77	
		1418.79 (bending)	3185.11 r1 as					
	III	3584.60 (stretching)		3193.34 r2 ss	3128.57	1675.05	1558.61	675.51
				3192.44 r1 ss				
			1441.87 (bending)	3185.85 r1 as				
			3183.97 r2 as					
IV	3593.59 (stretching)		3192.13 r1 ss	3128.16	1675.57	1571.98	666.86	
		1429.76 (bending)	3191.30 r2 ss					
			3184.96 r1 as					
			3178.93 r2 as					
			3176.47 r1 as					
B3PW91/cc-pvtz	I	3557.32 (stretching)	3201.02 r1 ss	3137.76	1694.02	1580.98	688.28	
		1424.70 (bending)	3192.44 r1 as					
			3185.18 r1 as					
	II	3591.71 (stretching)	3201.87 r1 ss	3138.13	1694.12	1585.83	686.24	
		1428.82 (bending)	3192.88 r1 as					
	III	3606.48 (stretching)		3201.50 r2 ss	3137.19	1688.43	1575.14	691.76
				3200.13 r1 ss				
			1438.23 (bending)	3192.43 r1 as				
			3191.96 r2 as					
IV	3616.81 (stretching)		3184.35 r1 as	3137.05	1689.25	1585.64	685.62	
		1429.70 (bending)	3199.94 r1 ss					
			3199.47 r2 ss					
			3192.07 r1 as					
			3187.11 r2 as					
			3184.23 r1 as					

r1: ring 1, r2: ring 2, ss: symmetric stretching, as: asymmetric stretching

The C–S–C and C–N oscillation frequencies were not significantly affected by the change in functional groups. The theoretical calculations showed that the C=C oscillations were the same for compounds I and II ( $1679 \text{ cm}^{-1}$ ); i.e.  $\text{NO}_2$  and Cl did not alter these oscillations. A similar case was observed for compounds III and IV. In addition, aliphatic C–H vibrations were calculated as  $3128 \text{ cm}^{-1}$  for all the compounds.

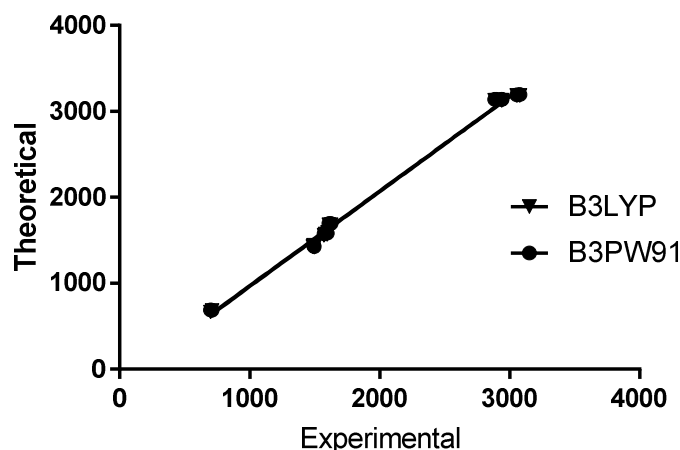


Figure 3. Linear regression for the experimental and theoretical calculations.

Comparing compounds I and II, NO<sub>2</sub>, which has a high electronegativity, caused a bathochromic shift in the absorption wavelength of compound II. Furthermore, a single peak was observed in the experimental spectrum of compound II, but two peaks were obtained from the theoretical calculations (experimental: 368.5 nm, theoretical: 328.4 and 405.57 nm for B3PW91; 333.43 and 411.11 nm for B3LYP, Table 4). Experimentally, these peaks were likely superimposed and a single peak was observed; the mean of the theoretically obtained peaks was consistent with the experimental results. Also, there was an inverse relationship between the HOMO–LUMO energy gap ( $\Delta E$ ) and the absorption wavelengths: the absorption wavelength of II, which was the longest, had the smallest  $\Delta E$  and the absorption of the III, shorter wavelength, had the largest  $\Delta E$ . The CH<sub>2</sub> substituent caused compound IV to have the lowest electronegativity thus the absorption was bathochromically shifted.

Table 7. Theoretical <sup>1</sup>H-NMR data of compounds I–IV ( $\delta$ , ppm, DMSO-d<sub>6</sub>).

Method	Comp.	$\delta$ Aliphatic-H	$\delta$ Aromatic-H	$\delta$ N-H	$\delta$ ethylenic C-H	
B3LYP/cc-pvtz	I	2.25 2.48 3.09	(s, 3H -CH <sub>3</sub> )	7.46-8.00 (8H, aromatic)	8.33 (g, -NH)	7.54 (s, 1H)
	II	2.27 2.48 3.11	(s, 3H -CH <sub>3</sub> )	7.30-8.72 (9H, aromatic)	8.28 (g, -NH)	7.61 (s, 1H)
	III	2.17, 2.46, 3.04 4.29, 4.39	(s, 3H -CH <sub>3</sub> ) (s, 2H -CH <sub>2</sub> -)	7.80-7.97 (10H, aromatic)	5.09 (g, -NH)	7.44 (s, 1H)
	IV	2.22, 2.35, 3.75 2.82, 3.09 3.11, 3.52	(s, 3H -CH <sub>3</sub> ) (t, 2H -CH <sub>2</sub> -) (t, 2H -CH <sub>2</sub> -)	7.48-7.97 (10H, aromatic)	5.58 (g, -NH)	7.35 (s, 1H)
B3PW91/cc-pvtz	I	2.40 2.60 3.21	(s, 3H -CH <sub>3</sub> )	7.66-8.20 (8H, aromatic)	8.57 (g, -NH)	7.70 (s, 1H)
	II	2.43 2.60 3.23	(s, 3H -CH <sub>3</sub> )	7.47-8.89 (9H, aromatic)	8.44 (g, -NH)	7.77 (s, 1H)
	III	2.32, 2.59, 3.16 4.43, 4.53	(s, 3H -CH <sub>3</sub> ) (s, 2H -CH <sub>2</sub> -)	7.97-8.15 (10H, aromatic)	5.29 (g, -NH)	7.60 (s, 1H)
	IV	2.33, 2.54, 3.19 2.98, 3.22 3.21, 3.62	(s, 3H -CH <sub>3</sub> ) (t, 2H -CH <sub>2</sub> -) (t, 2H -CH <sub>2</sub> -)	7.70-8.19 (10H, aromatic)	5.71 (g, -NH)	7.52 (s, 1H)

The calculated hydrogen chemical shifts were compared to the experimental values, as shown in Table 7. Experimental chemical shifts were obtained in DMSO. There is good agreement between the theoretical and experimental values, as seen in Figure 4. The Pearson correlation coefficients of the NMR data mean values were  $R=0.7479$  and  $R=0.7490$  for B3LYP and B3PW91, respectively. Although there was a strong correlation between them, there was a slight difference for the experimental and theoretical  $\delta_{N-H}$  values (Figure 4). The proton chemical shift was affected by intramolecular hydrogen bond interactions, especially for hydrogens bound to an electronegative atom or groups of atoms, as observed for the  $\delta_{N-H}$  shifts.

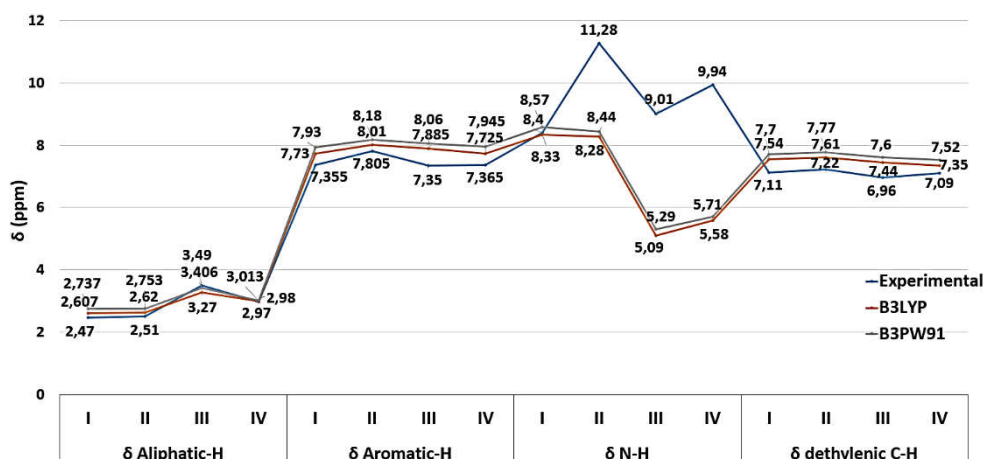


Figure 4. Experimental results plotted against the theoretical calculations for  $^1\text{H-NMR}$ .

The  $^{13}\text{C-NMR}$  calculations were in good agreement with the experimental results. The B3LYP calculations yield results lower than those of B3PW91 although there was a very close linear relationship between the experimental results and the theoretical calculations. Comparative results for compound I are given in Figure 5.

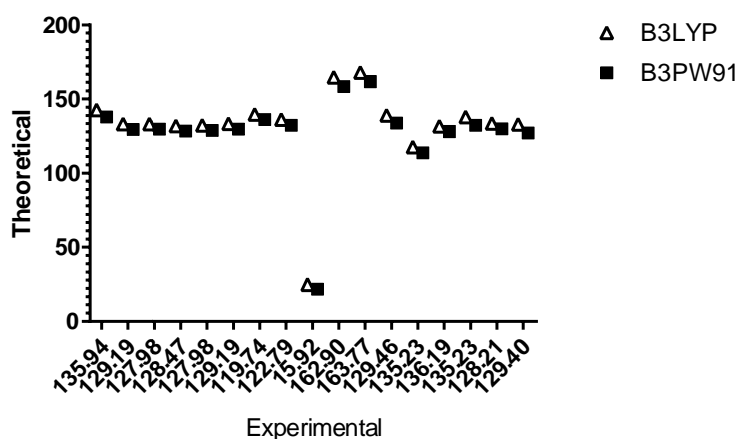


Figure 5. Experimental and calculated  $^{13}\text{C-NMR}$  data for compound I.

The calculated carbon chemical shifts of compounds I–IV are shown in Table 8. The Pearson correlation  $R$  is between 0.9687 and 0.9983. In this case, both calculation methods were equally successful.

Table 8. <sup>13</sup>C-NMR data of compounds I–IV (δ, ppm, DMSO-d<sub>6</sub>); TMS standard 182.4656. Method used B3LYP/6-311+G(2d,p).

	B3lyp/cc-pvtz				B3PW91/cc-pvtz			
	I	II	III	IV	I	II	III	IV
C <sub>1</sub>	142.55	142.23	142.56	142.95	137.88	137.66	137.99	138.56
C <sub>2</sub>	133.10	132.92	132.65	133.41	129.40	129.20	128.90	129.39
C <sub>3</sub>	133.27	133.40	132.74	132.63	129.80	129.93	129.25	129.28
C <sub>4</sub>	131.95	132.20	131.69	131.48	128.46	128.73	128.19	128.07
C <sub>5</sub>	132.18	132.32	132.10	131.51	128.68	128.90	128.56	128.31
C <sub>6</sub>	133.41	133.70	134.00	134.17	129.79	130.16	130.41	130.37
C <sub>7</sub>	139.59	140.69	137.51	136.44	136.22	137.33	133.97	132.84
C <sub>8</sub>	136.24	136.15	137.08	136.56	132.23	132.14	132.97	132.90
C <sub>9</sub>	24.99	24.87	24.97	25.53	21.70	21.54	21.66	21.73
C <sub>10</sub>	164.67	166.79	162.68	163.29	158.41	160.45	156.10	156.23
C <sub>11</sub>	167.90	167.25	175.65	176.44	161.74	161.25	169.87	170.16
C <sub>12</sub>	138.88	149.05	142.20	144.60	133.81	143.72	137.53	139.54
C <sub>13</sub>	117.60	113.44	132.89	132.62	113.77	110.00	129.20	128.79
C <sub>14</sub>	131.82	131.08	132.02	132.17	128.13	127.45	128.46	128.61
C <sub>15</sub>	137.94	145.48	132.26	129.83	132.19	140.29	128.55	126.25
C <sub>16</sub>	133.52	130.62	132.57	132.28	129.88	127.05	128.97	128.79
C <sub>17</sub>	132.97	120.69	133.47	132.88	127.00	117.18	129.49	129.34
C <sub>18</sub>	-	-	54.16	53.47, 38.72	-	-	50.09	48.85, 34.53
R	0.9687	0.9914	0.9982	0.9980	0.9675	0.9914	0.9978	0.9983

R: The Pearson correlation coefficients for experimental result vs theoretical calculations

#### 4. Conclusion

In this study, four new substituted 1,3,4-thiadiazole compounds derived from  $\alpha$ -methyl cinnamic acid were synthesised and their structures were characterised using FT-IR, <sup>1</sup>H-NMR and <sup>13</sup>C-NMR spectroscopy. The UV-Vis absorption properties were also studied. The spectroscopic data show that the expected compounds were obtained. The theoretical calculations and experimental results were in good agreement; the theoretical methods were particularly successful for the C-NMR and IR analyses. The solvents used for the UV experiments affected the absorption wavelength. Furthermore, the electronegativity of the substituents played a key role in the chemical and electronic properties, from chemical hardness to the energy band gap  $\Delta E$ . From the different methods used for the calculations, B3LYP was the best choice both in terms of calculation time and accuracy.

#### References

- [1] Şener, N. and Gür, M., Novel 1,3,4-thiadiazole compounds derived from 4-phenylbutyric acid: Synthesis, characterization and DFT studies, **Journal of Balıkesir University Institute of Science and Technology**, DOI: 10.25092/baunfbed.343149
- [2] Gür, M. and Şener, N., Synthesis and Characterization Of Some New 1,3,4-Thiadiazole Compounds Derived From  $\alpha$ -Methyl Cinnamic Acid and Their Energetics and Spectral Analyses Based on Density Functional Theory Calculations, **Anadolu University Journal of Science and Technology, A-Applied Sciences and Engineering**, DOI: 10.18038/aubtda.310899

- [3] Jaiswal, S. and Sigh, S., A novel POCl<sub>3</sub> catalysed expeditious synthesis and antimicrobial activities of 5-substituted-2-arylbenzalamino-1,3,4-thiadiazole, **International Journal of Engineering Research and General Science**, 2, 6, (2014).
- [4] Ahmed, M., Jahan, J. and Banco S., A simple spectrophotometric methods for the determination of copper in industrial, environmental, biological and soil, samples using 2, 5-dimercapto 1, 3, 4-thiadiazole, **Journal of Analytical Science and Technology**, 18, 805-810, (2002).
- [5] Aliabadi, A., Eghbalian, E. and Kiani, A., Synthesis and evaluation of the cytotoxicity of a series of 1,3,4-thiadiazole based compounds as anticancer agents, **Iranian Journal of Basic Medical Sciences**, 16, 1133-1138, (2013).
- [6] Young, G. and Eyre, W., III. -Oxidation of benzalthiosemicarbazone, **Journal of the Chemical Society**, 79: 54-60, (1901).
- [7] Freund, M. and Meinecke, C., Uber derivate des thiobiazolins, **Chemische Berichte**, 29, 2511-2517, (1896).
- [8] Praphulla, C.G., Constitution of the so-called dithio-urazole of martin freund. ii. New methods of synthesis, isomerism and poly-derivatives, **Journal of the American Chemical Society**, 44 (7), 1510-1517, (1922).
- [9] Hamama, W.S., Gouda, M.A., Abd-El-Wahab, M.H. and Zoorob, H.H., Recent advances in the chemistry and synthetic uses of amino-1,3,4-thiadiazoles, **Journal of Heterocyclic Chemistry**, 51: 1558–1581, (2014).
- [10] Kuz'Mich, N.N., Lalaev, B.Y., Yakovlev, I.P., Semakova, T.L. and Zakhs, V.E., Thiobenzohydrazides and dithiocarbazates in the synthesis of new 1,3,4-thiadiazine and 1,3,4-thiadiazole derivatives, **Russian Journal of General Chemistry**, 79: 7: 1583–1584, (2009).
- [11] Young, R.W. and Wood, K.H., The cyclization of 3-acyldithiocarbazate esters, **Journal of the American Chemical Society**, 77 (2), 400-403, (1955).
- [12] Ainsworth, C., The condensation of aryl carboxylic acid hydrazides with orthoesters, **Journal of the American Chemical Society**, 77 (5): 1148-1150, (1955).
- [13] Gray, C.J. and Parker, R.C., The Synthesis of an  $\alpha$ -Azaornithine Derivative and its Reaction with Ttrypsin, **Tetrahedron**, 31, 2940-2943, (1975).
- [14] Guha, P.J., Ring closure of hydrazodithio- and -Monothio-Dicarbonamides with acetic anhydride, **Journal of the American Chemical Society**, 45, 1036, (1923).
- [15] Xuan, L., Song, Z., Yi-Ming, J., Guang-Zhao, L., Liang, J., Xiao, L., Qiu-Lei, X. and You-Xuan, Z., Syntheses, crystal structure and photophysical property of iridium complexes with 1,3,4-oxadiazole and 1,3,4-thiadiazole derivatives as ancillary ligands, **Journal of Organometallic Chemistry**, 785, 11-18, (2015).
- [16] Ruangchai, T., Siriporn, J. and Visit, V., Computational calculations of substitution pattern effects on the optical properties of benzobis (thiadiazole) derivatives as near-infrared-emitting organic compounds, **Computational and Theoretical Chemistry**, 1098, 31–40, (2016).
- [17] Tarek, A.M., Ahmed, E.H., Ibrahim, A.S., Ahmed, M.A. and Wajdi M.Z., Conformational stability, spectral analysis (infrared, Raman and NMR) and DFT calculations of 2-Amino-5-(ethylthio)-1,3,4-thiadiazole, **Journal of Molecular Structure**, 1130, 434-441, (2017).
- [18] Gür, M., Muğlu, H., Çavus M.S., Güder, A., Sayıner, H.S. and Kandemirli, F., Synthesis, characterization, quantum chemical calculations and evaluation of

- antioxidant properties of 1,3,4-thiadiazole derivatives including 2- and 3-methoxy cinnamic acids, **Journal of Molecular Structure**, 1134, 40-50, (2017).
- [19] Gür, M., Şener, N., Muğlu, H., Çavuş, M.S., Özkan, O.E., Kandemirli, F. and Şener, İ., New 1,3,4-thiadiazole compounds including pyrazine moiety: Synthesis, structural properties and antimicrobial features, **Journal of Molecular Structure**, 1139, 111-118, (2017).
- [20] Er, M., Isildak, G., Tahtacı, H. and Karakurt, T., Novel 2-amino-1,3,4-thiadiazoles and their acyl derivatives: Synthesis, structural characterization, molecular docking studies and comparison of experimental and computational results, **Journal of Molecular Structure**, 1110, 102-113, (2016).
- [21] Hohenberg, P. and Kohn, W., Inhomogeneous electron gas, **Physical Review Letters**, 136, B864–B871, (1964).
- [22] Kohn, W. and Sham, L., Self-consistent equations including exchange and correlation effects, **Physical Review Letters**, 140, A1133–A1138, (1965).
- [23] Gaussian 09, Revision B.01, Frisch M. J.; Trucks G. W.; Schlegel H. B.; Scuseria G. E.; Robb M. A.; Cheeseman J. R.; Scalmani G.; Barone V.; Mennucci B.; Petersson G. A.; Nakatsuji H.; Caricato M.; Li X.; Hratchian H. P.; Izmaylov A. F.; Bloino J.; Zheng G.; Sonnenberg J. L.; Hada M.; Ehara M.; Toyota K.; Fukuda R.; Hasegawa J.; Ishida M.; Nakajima T.; Honda Y.; Kitao O.; Nakai H.; Vreven T.; Montgomery J. A.; Jr.; Peralta J. E.; Ogliaro F.; Bearpark M.; Heyd J. J.; Brothers E.; Kudin K. N.; Staroverov V. N.; Keith T.; Kobayashi R.; Normand J.; Raghavachari K.; Rendell A.; Burant J. C.; Iyengar S. S.; Tomasi J.; Cossi M.; Rega N.; Millam J. M.; Klene M.; Knox J. E.; Cross J. B.; Bakken V.; Adamo C.; Jaramillo J.; Gomperts R.; Stratmann R. E.; Yazyev O.; Austin A. J.; Cammi R.; Pomelli C.; Ochterski J. W.; Martin R. L.; Morokuma K.; Zakrzewski V. G.; Voth G. A.; Salvador P.; Dannenberg J. J.; Dapprich S.; Daniels A. D.; Farkas O.; Foresman J. B.; Ortiz J. V.; Cioslowski J.; Fox D. J., Gaussian, Inc., Wallingford CT, (2010).